

Schrödinger Cat State Spectroscopy—A New Frontier for Analytical Chemistry

John C. Wright*

Cite This: *Anal. Chem.* 2020, 92, 8638–8643

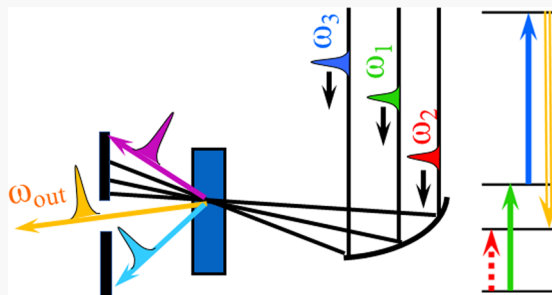
Read Online

ACCESS |

Metrics & More

Article Recommendations

ABSTRACT: The invention of the laser generated great excitement, because its ability to create quantum state coherences could form a new family of coherent spectroscopies that were the optical analogue of multidimensional nuclear magnetic resonance (NMR). The full realization of this promise has not yet been realized, but the pathway forward is clear. The path involves the use of multiple, tunable lasers that create a Schrödinger cat state, where the system is simultaneously in a mixture of vibrational and/or electronic states. The multiplicity of these states confers many advantages for analytical methods: high selectivity from the multiple spectral dimensions, line-narrowing, isolation of spectral features where quantum states are coupled, and spectral decongestion. Now that the feasibility of Schrödinger cat spectroscopy has been demonstrated, the future is open for the development of a new frontier in analytical chemistry that creates a new set of tools for studying the complex systems that form the heart of analytical chemistry.



This Perspective describes a new frontier for analytical chemistry that is based on the emergence of a family of fully coherent nonlinear spectroscopies that complement existing incoherent spectroscopies.¹ Optical spectroscopy is already a dominant methodology for chemical measurement, because it provides direct measurement of the vibrational and electronic states of the individual molecules in a sample at the most fundamental quantum mechanical level. Coherent spectroscopies have many similarities to incoherent spectroscopies. In fact, the basis of all spectroscopy is the creation of a coherence of quantum states by an electromagnetic field.² The electric (most spectroscopies) or magnetic (NMR) field component of light entangles molecular states to form a coherence, i.e., a superposition state where the molecule is in two states simultaneously. Schrödinger's cat state is a famous example of a coherence where the cat in a box is simultaneously dead and alive.³ The cat state collapses to dead or alive when the box is opened. A coherence is time dependent and oscillates at the frequency difference between the two entangled states. Any time charges oscillate, they emit light. Coherent spectroscopies use multiple pulses to create and manipulate a series of coherences until the time when the chaotic environment collapses the cat states (dephasing) and populates one of its entangled states. Incoherent spectroscopies are based on using the resulting population after the collapse. Refraction, absorption, emission, and Raman are all the result of coherences and collapsed state populations.

The new coherent spectroscopies result from having more than two states entangled. It is then a multiple quantum coherence (MQC). MQCs form the heart of NMR methods

where the coherences are superpositions of up and down nuclear spin states. The wave function for any MQC is $\Psi(\vec{x}, t) = \sum_{n=\text{coupled states}} c_n(t) \psi_n(\vec{x}) e^{i(\vec{k}_n \vec{z} - \omega_n t)}$ where c_n is the amplitude of state n , and $k \equiv \frac{2\pi}{\lambda}$ and ω define its spatial and temporal oscillations. The states can be nuclear, rotational, vibrational, and electronic. The oscillation frequencies occur at all frequency combinations of the states in the MQC. Their re-emission is cooperative and directional because of constructive interference in particular directions defined by momentum conservation. Coherences exist while the electric or magnetic parts of the electromagnetic excitation fields drive the molecular transitions and the light they emit. After the excitation fields disappear, the coherences undergo free induction decay (FID), because interactions with the chaotic thermal environment destroy the phase relationships. Dephasing causes the cat state to collapse, and the emission then becomes incoherent and random.⁴ The FID time scales are femtoseconds for electronic coherences, picoseconds for vibrational coherences, and milliseconds for NMR coherences. So all coherent spectroscopies must emit during those time scales. That requires high instantaneous intensities and short pulses but not too short.

Received: April 17, 2020

Accepted: June 4, 2020

Published: June 4, 2020



It is also important to recognize that the states comprising the cat state must be coupled in order to have an output intensity.⁵ Without coupling, they would lack the dipole moment that is necessary for emission. Coupling occurs when the excitation of a state perturbs the optical properties of other states. Combination band and overtone states are examples of coupling where new frequencies appear because there are transition dipoles involving the coupled states. The coupling requirement provides a great deal of selectivity for measurements of complex systems, because the only cross-peaks that arise in experiments must be from coupled states. The coupling requirement is a powerful approach for removing spectral congestion.⁶ Similar concepts are responsible for NMR cross-peaks.⁷

These same ideas form the basis for fluorescence and Raman spectroscopy but in a very strange way. Fluorescence and Raman are based on populations that result from the collapse of a cat state created by an electromagnetic field. The strangeness results because the fluctuations of the vacuum also create coherences by stimulating a transition. Light is quantized, and quantum mechanics demands that everything obeys an uncertainty principle. If the vacuum had no energy, the energy would be exactly zero and would therefore violate the uncertainty principle. Therefore, the vacuum must have a “zero-point fluctuation” involving all particles and photons.⁸ Fluorescence and Raman spectroscopy are both based on the creation of a cat state by an electromagnetic field. They differ in when the vacuum fluctuations induce the output transition. Raman transitions occur when the vacuum stimulates emission before the cat state collapses, while fluorescence transitions occur after the cat state collapses and forms an excited state population. In both cases, the electronic and vibrational states involved in these transitions must be coupled. The bonds that are changing in a vibrational mode are also affecting the specific electronic states created by those bonds.

The incredible power of spectroscopic techniques becomes compromised in complex samples when spectral congestion obscures the individual spectral features. NMR solves this problem by creating MQCs of ¹H, ¹³C, ³¹P, etc. nuclear spin states.⁹ The states in the MQCs that are coupled by interactions create cross-peaks in multidimensional spectra. The high selectivity of NMR MQCs rests both on the multidimensionality of the spectra and the coupling requirement that drastically reduces spectral congestion and identifies interacting states. Why cannot we transfer these ideas to other spectroscopies? After all, there was great excitement after the laser was invented, because it had the coherence required to create coherences of electronic and vibrational states that would be analogous to NMR’s spin states.¹⁰ The very fast dephasing times of vibrational and electronic states have prevented implementation of the optical analogues for a long time, but the development of different approaches and technologies has now opened this new field.¹

■ BACKGROUND

Coherent multidimensional spectroscopy (CMDS) is based upon forming Schrödinger cat states by exciting multiple vibrational and electronic states on time scales that are short or comparable to the dephasing time scales.⁴ The cat states re-emit beams at all frequency combinations of the resonant excitation beams. Angling the excitation beams forces the constructive interference between the molecules in the excitation region to occur in different directions for each frequency combination.¹ Figure 1 illustrates a typical CMDS

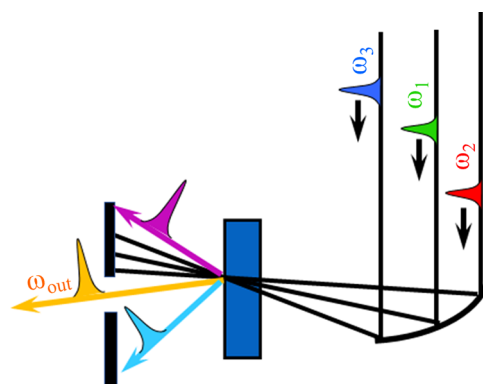


Figure 1. Three tunable excitation pulses excite multiple quantum coherences in a sample. Pairs of coherences create new beams at frequency sums and differences of the excitation pulses. Emission from one pair is chosen for measurement.

experiment. Three coherent excitation pulses with frequencies ω_1 , ω_2 , and ω_3 and interpulse time delays τ_{21} and τ_{31} are focused into a sample, where they excite a cat state that entangles three vibrational and/or electronic states with the ground state. The angles between pulses define the directions for constructive interference that allows angular resolution of each output beam.

Frequency domain CMDS measures the resonant enhancement that occurs as the excitation frequencies are scanned, while time domain CMDS measures the phase modulations of the coherences in the cat state by scanning the time delay between excitation pulses. Frequency domain CMDS evolved from the field of coherent Raman spectroscopy, where coherent anti-Stokes Raman spectroscopy (CARS) played a dominant role.¹¹ Time domain CMDS evolved from the field of ultrafast spectroscopy, where pump–probe and photon echo played dominant roles.¹²

■ CMDS EXAMPLES

Vibrational spectroscopies take advantage of the selectivity provided by sharp spectral features, while electronic spectroscopies take advantage of the low detection limits provided by their large transition moments.⁵ Methods like resonance Raman combine both advantages. CMDS methods add additional resonances that provide greater selectivity. Doubly vibrationally enhanced (DOVE) CMDS is a typical multidimensional method that uses three picosecond pulses with frequencies ω_1 , ω_2 , and ω_3 . The pulses are focused into a sample where they excite three quantum states. The quantum states are a vibrational mode, v , a combination band, $(v+v')$, and a real or virtual electronic state, (e) . The resulting Schrödinger cat state oscillates at the frequency differences between all combinations of the g , v , $v+v'$, and e . An oscillating transition dipole emits light beams at each of these frequencies. For DOVE CMDS, it is $\omega_{\text{out}} = \omega_1 - \omega_2 + \omega_3$. Since all of the molecules in the excitation region are excited by the same electromagnetic fields, the phases of their oscillations are correlated and can cooperatively emit light beams in directions defined by the vector addition of the three excitation and output photons’ k -vectors. In these directions, the spatial phase oscillations of the coherences and excitation pulses are matched, so they constructively interfere. For DOVE CMDS, the condition for phase matching is $\vec{k}_{\text{out}} = \vec{k}_1 - \vec{k}_2 + \vec{k}_3$. Choosing spatial geometries that meet this phase matching condition results in a series of output beams with different frequencies and angular separations. Frequency

domain CMDS measures the intensity of an output beam as a function of ω_1 , ω_2 , and ω_3 . When the frequencies are resonant with vibrational and/or electronic transitions, the output intensity increases multiplicatively for each additional resonance. Time domain CMDS overlaps an output beam with another beam that serves as a local oscillator. The local oscillator heterodynes with the beam to create a difference frequency that is then measured. The heterodyne detection is identical to that used for radio, television, and NMR.

A specific example of the selectivity of frequency domain CMDS is a recent experiment on drug–substrate binding done by David Klug’s group at Imperial College.¹³ The drug is SU5402, a potent and selective inhibitor of the target protein, a fibroblast growth factor receptor (FGFR). Figure 2 shows the

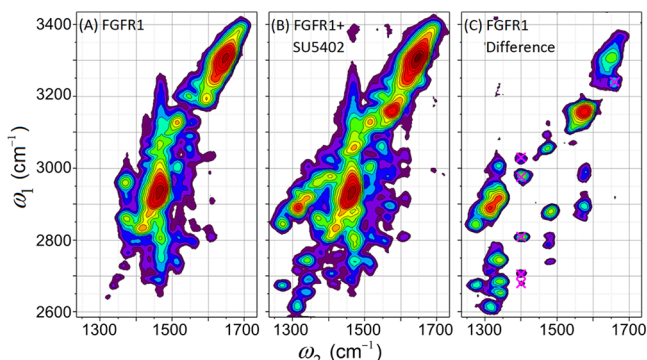


Figure 2. DOVE 2D spectra of a target protein (A), drug–protein target complex (B), and their difference.¹³ The pink crosses in C denote vibrational modes associated with the drug–target binding. The x- and y-axes denote the two excitation frequencies. The color bar denotes the output intensity. Adapted with permission from ref 13. Copyright (2019) American Chemical Society.

two-dimensional (2D), DOVE spectrum of the drug, the drug–target complex, and the difference spectrum. Each was acquired by exciting two vibrational modes and virtual electronic states of the drug–target complex. The color map in the figure represents the output intensity, as ω_1 and ω_2 become resonant with the ν and $\nu+\nu'$ modes. The three spectra show the cross-peaks between the fundamental vibrational modes (x-axis) and the corresponding overtone and combination bands (y-axis) of the protein target alone (A), the drug and protein target (B), and the difference spectrum (C). The protein target spectrum (A) has over ~200 peaks. The drug–target spectrum (B) has an additional 63 peaks that are resolved in the difference spectrum (C). The pink crosses identify 6 peaks in the difference spectrum that arise specifically from drug–target binding where the protein and drug modes are coupled by the binding. The presence of cross-peaks between drug and target ensures that they arise from the interactions binding them.

The DOVE spectroscopy in this example uses the ω_1 , ω_2 , and ω_3 pulses to create an output beam at $\omega_{\text{out}} = \omega_1 - \omega_2 + \omega_3$ and measures the intensity as a function of ω_1 and ω_2 with ω_3 constant.^{6,11,14–18} The arrows in Figure 3a show the time ordering of the three resonances from left to right that create the coherence between states e and ν that emit the output signal. Note that the first two interactions excite a vibrational mode and a combination band, while the third interaction creates the output signal. The sequence of resonances required to create the $e\nu$ coherence that emits the output signal is $gg \rightarrow gv \rightarrow (\nu + \nu')$, $\nu \rightarrow (e + \nu)$, $\nu \xrightarrow{\text{out}} \nu\nu$, where the first

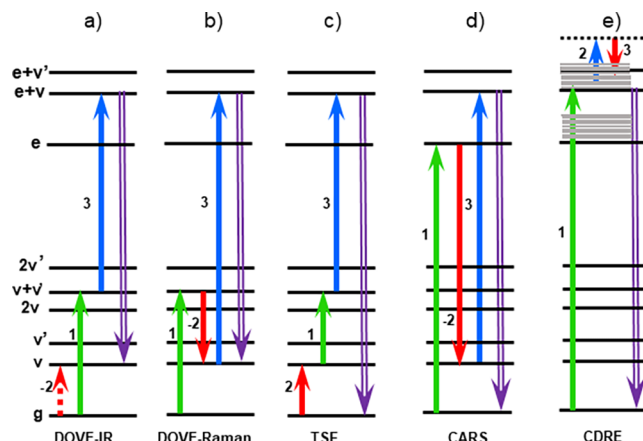


Figure 3. Representative coherence pathways for fully coherent CMDS. The arrows denote the vibrational (ν and ν') and electronic (e) transitions created by the three excitation pulses. The numbers denote their frequencies. The time ordering of the pulses proceeds from left to right. The last arrow denotes the emission. Rotational states are added in part (e) to highlight their role in the process.

letters denote the sequence of states resulting in state e of the output coherence, and the second letters denote the sequence that creates state ν . The pathway is a hybrid between infrared absorption (the first two interactions) and Raman experiments (the last two interactions). Note that the IR interactions create coherences involving fundamental and combination band state transitions that are allowed and formally forbidden, respectively. The coupling requirement is manifested in allowing a combination band transition. Figure 3b shows a similar DOVE pathway that can be considered a vibrationally resonant Raman process involving the pathway $gg \xrightarrow{1} (\nu + \nu')$, $g \xrightarrow{-2} \nu' g \xrightarrow{3} eg \xrightarrow{\text{out}} gg$. The two differ in the time ordering of the first two excitation fields.

In addition, DOVE and other fully coherent spectroscopies are capable of line-narrowing and resolving spectral structures lying beneath inhomogeneously broadened spectra.^{19–21} Their ability to resolve these underlying structures rests on the establishment of multiple resonances with a specific component of the inhomogeneous system. The multiplicative resonance enhancements lift the intensity of the fully resonant component well above other components of the system, which have fewer resonances.

DOVE spectroscopy is one example of a frequency domain CMDS method, but there are others that differ only in the wavelengths and time orderings of the three excitation pulses and the quantum states that are accessed. Figure 3b–e shows four additional examples. Triple sum frequency (TSF) spectroscopy is a similar method to DOVE spectroscopy.^{22–25} The sequence of resonances for TSF is $gg \xrightarrow{2} vg \xrightarrow{1} (\nu + \nu')$, $g \xrightarrow{3} (e + \nu')$, $g \xrightarrow{\text{out}} gg$. Just like DOVE spectroscopy, the first two interactions create a coherence involving fundamental and combination band modes, but in this case, the infrared transitions are all allowed. Also, like DOVE spectroscopy, the last two interactions create a Raman transition. In this case, the Raman transition involves a combination band that is formally forbidden. The coupling requirement is therefore manifested in the Raman transition. Coherent anti-Stokes Raman spectroscopy (CARS) was the first member of the fully coherent family²⁶ and is based on the pathway

$g\overset{1}{g}\rightarrow e\overset{2}{g}\rightarrow v\overset{3}{g}\rightarrow(e+v')$, $g\overset{\text{out}}{\rightarrow}gg$, where all of the interactions are Raman transitions. It provides complementary selection rules to DOVE and TSF spectroscopies.^{27,28} The last example is coherent doubly resonant electronic spectroscopy (CDRES).²⁹ It is based on pathways involving electronic, vibrational, and rotational states, $g\overset{1}{g}\rightarrow(e+v+J)$, $g\overset{2}{\rightarrow}e'g\overset{3}{\rightarrow}(e+v+J')$, $g\overset{\text{out}}{\rightarrow}gg$. It achieves the remarkable resolution of the thousands to millions of vibrational and rotational states characteristic of gas phase molecules that make optical rotational spectroscopy feasible. Figure 4 shows an expanded view of a narrow range of the 2D

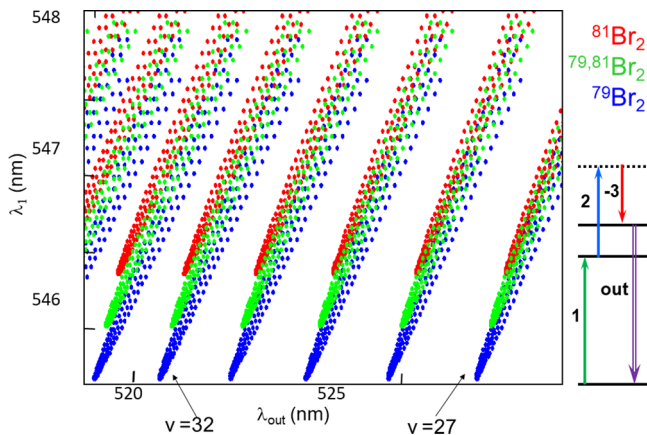


Figure 4. 2D CDRES spectrum of bromine isotopomers. The second and third interactions involve a virtual state (i.e., a nonresonant electronic state). Adapted with permission from ref 29. Copyright (2008) American Chemical Society.

vibrational and rotationally resolved spectral features of the three isotopomers of gaseous bromine. Even within this limited range, there are $\sim 17\,000$ features. First, a narrow-band, tunable laser at λ_1 excites a specific vibrational/rotational state of the excited electronic state. A broad-band infrared excitation provides the next two interactions that together excite a different vibrational/rotational state. A high-resolution monochromator then resolves all the output transitions at λ_{out} .

■ NEW FRONTIERS FOR CMDS IN ANALYTICAL CHEMISTRY

These examples are representative of frequency domain CMDS. An alternative approach is time domain CMDS.^{12,30} Rather than scanning over a resonance, time domain methods scan the time delays between pulses relative to a local oscillator in order to resolve the phase oscillations of each coherence. This approach mirrors current NMR methods. Fourier transforms convert the phase oscillations into the corresponding frequencies. Time domain CMDS has become an important method in physical chemistry for measuring chemical dynamics in simple systems, but it has not been important in analytical chemistry for measuring the spectra of complex systems. There are four central problems that constrain both approaches and their widespread dissemination.

(1) For frequency domain CMDS, it is difficult to continuously scan ultrafast lasers over the wide range of wavelengths required for analytical applications. Commercial laser systems are designed to go to a specific wavelength and measure the transient dynamics. The

software and hardware for commercial systems must be modified by the user in order to scan the frequencies needed to perform frequency domain experiments. For time domain CMDS, the accessible spectral regions are sharply limited by the bandwidth of the short excitation pulses. Expanding the bandwidth results in pulses that are too short to create substantial coherence amplitudes.³¹ NMR methods avoid this problem by increasing the excitation intensity. This strategy is not possible for time domain CMDS, because the required intensities would destroy the sample.

- (2) For both approaches, the detection limits are usually set by the nonresonant background that results from the same virtual electronic states controlling the index of refraction.²⁸ Current technology allows millimolar detection limits.
- (3) Time domain CMDS is sensitive only to the strongest vibrational modes.³¹
- (4) The fundamental concepts involved in Schrödinger cat state spectroscopies are foreign to most scientists, because current academic curricula do not include coherent phenomena. In addition, phase matching and temporal and spatial overlap considerations are unforgiving, and workers must be careful to ensure their optimization. It therefore becomes a daunting but rewarding effort to enter into this emerging field.

These problems are solvable if there is a motivation to solve them. The following are examples of how these problems can be solved.

- (1) Commercial laser systems rely on nonlinear processes for changing the wavelength. Scanning the excitation and detection frequencies requires changing multiple nonlinear crystal angles, excitation pulse time delays, and beam directions in order to preserve phase matching and temporal and spatial overlap. Our program has shown that these changes can be automated, so 3D spectra can be acquired without spectral artifacts.²⁵ Commercial systems can also be automated if there is a market that justifies it. Analytical chemists know the applications and can create this new market and the instruments and strategies that meet its demands.
- (2) The virtual states that create the nonresonant background exist only during the time that all excitation pulses are temporally overlapped. Introducing a time delay between excitation pulses can eliminate the nonresonant background.³² The vibrational and electronic state coherences, however, persist until dephasing occurs. The time delays can be extended to provide even great discrimination against nonresonant background if the duty cycle is increased by using high-repetition-rate lasers. Optical parametric oscillators are currently available with repetition rates $80\,000\times$ higher than the typical optical parametric amplifiers currently used.
- (3) Time domain CMDS is based on using the shortest femtosecond excitation pulses in order to resolve dynamics on the fastest time scales. Vibrational state transitions are very narrow, because they have long dephasing times. As a result, they require long pulses in order to build up the amplitude of vibrational states. Femtosecond pulses are so short that there is not adequate time to create vibrational coherences unless the vibrational modes have large transition moments.³³

The best compromise is using pulse widths that are comparable to the dephasing times so the spectral resolution and the discrimination against nonresonant background are both enhanced.

(4) Coherent phenomena and cat states form the heart of the emerging field of quantum computing and quantum technologies, and it is crucial for the academic curriculum and analytical chemistry in particular to embrace the coherent phenomena that underlie all of spectroscopy and technology. Computers play an important role in this expansion of the curricula, because the full use of Schrödinger cat states creates large data sets, which require advanced computational methods for data interpretation.

■ APPLICATIONS AT THE FRONTIERS OF ANALYTICAL CHEMISTRY

Analytical chemistry is a diverse field with many opportunities for creativity. I highlight three examples.

(1) Most analytical applications address solving problems in complex samples. It is these applications where the selectivity of CMDS methods can make their greatest contributions. Figure 1 is a clear example of how multiple dimensions can resolve the spectral congestion of a complex protein and identify cross-peaks between different sample components that identify the quantum states associated with coupling between components. CMDS expands the capabilities of vibrational spectroscopy by providing multidimensional spectral fingerprints of specific molecular components.³⁴

(2) In microscopy, fluorescence labels are often used to enhance specific structures. Methods like CARS and stimulated Raman scattering (SRS) are label-free methods for providing contrast based on resolving characteristic vibrational modes.³⁵ Both approaches create 1D spectral fingerprints. CMDS methods are based on the same technology as CARS and SRS but also provide multidimensional spectral fingerprints that can greatly extend the capabilities of label-free imaging.

(3) Synthetic chemistry is based on creating and breaking bonds. Bonds are manipulated by combinations of bending, torsional, wagging, and stretching vibrational modes. The changes in bond energies are usually caused by asymmetrical vibrational modes that perturb electronic states and mix them with the ground electronic state. These effects are visualized by multidimensional reaction coordinate surfaces that show how the free energy depends on the coupled vibrational modes responsible for changes in bonding. Reaction surfaces of photochemical reactions have been directly measured in great detail by ultrafast spectroscopic variants of SRS.³⁶ However, most reactions occur on the ground electronic state surface. Fully coherent CMDS methods can directly measure the ground state reaction surface by resolving the coupled multidimensional vibrational modes and electronic states that define the reaction surface. In particular, the DOVE and TSF spectroscopies excite the asymmetric vibrational modes responsible for the reactions. These modes are not accessible with Raman based methods. Modes forming the reaction surface have large anharmonicities, because they change the bond energies and

consequently will have strong cross-peaks that identify their role in the reactions.

The anharmonicity and the potential energy reaction surface itself may also be directly measurable. When the excitation intensity creates Rabi frequencies that become comparable to the vibrational dephasing time, multiple interactions can occur during an individual excitation pulse so higher harmonics and combination bands can be excited. The excitations climb a vibrational ladder. The changes in frequency for the excitation measure the anharmonicity associated with each mode on the reaction surface. From this experiment, it is possible to directly measure the potential energy surface. Figure 5 shows the results

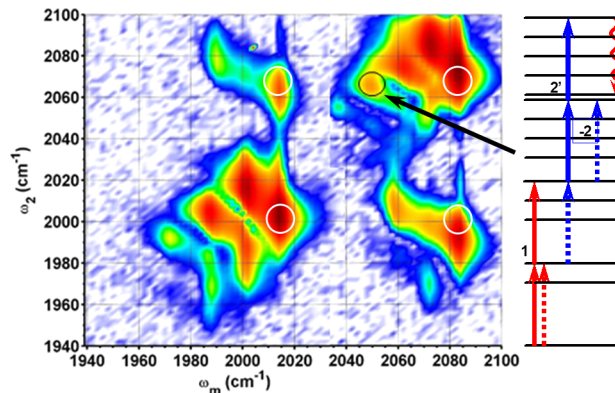


Figure 5. 2D DOVE spectrum of a rhodium dicarbonyl chelate.³¹ The diagram on the right shows the transitions created by the three tunable excitation pulses. The frequency of ω_1 was fixed near the transition to v' , while ω_2 was scanned (y-axis). The x-axis is the frequency of the output. White circles identify the diagonal and cross-peak frequencies that are present at low excitation intensity. The black circle identifies the feature created by the pathway on the right. The colors denote the output intensity. Adapted with permission from ref 37. Copyright (2010) American Chemical Society.

of a rhodium dicarbonyl molecule excited with high-intensity pulses.³⁷ At low intensities, the 2D spectrum contains the diagonal and cross-peaks for the symmetric and asymmetric C=O stretches. Their positions are highlighted by the white circles. At high intensities, the spectrum contains many more spectral features. Features appear for transitions involving $\Delta\nu = 0, 1, \dots, 6$ vibrational quantum numbers with each transition providing a value for the anharmonicity. The diagram shows an example of the resonances that create the feature highlighted by the black circle. All these features were fit within 2 cm^{-1} to a 2D Morse potential for the symmetric and asymmetric modes from $v = 0$ to 6. This ability to identify reaction surfaces can be a powerful tool for synthetic chemists to gain the insights required to understand reaction mechanisms at the most fundamental quantum mechanical level.

■ CONCLUSION

Fully coherent CMDS methods have the promise to create a powerful new analytical tool for solving problems in complex systems. Their high selectivity results from their ability to create multidimensional spectral fingerprints consisting of rotational, vibrational, and/or electronic states.^{25,34} As such, they embody aspects of infrared absorption, Raman, fluorescence, and UV/visible absorption spectroscopies. In addition to the multiple dimensions, the coupling requirement reduces the spectral congestion of complex materials by restricting the spectra to the

quantum states that are interacting. It is those states that are responsible for controlling the properties that are most useful to chemists.

This frontier is virgin territory. There is almost no CMDS work occurring outside of physical chemistry. Analytical chemistry is the field tasked with developing new chemical measurement technologies for tackling real world problems involving complex samples. It is analytical chemists who can lead this new frontier in developing these technologies and making CMDS reach its tremendous potential. Since recent experiments have demonstrated the feasibility of analytical applications, the field is now ready to further develop the technology so it will meet the requirements required of a versatile analytical methodology and to develop the applications that demonstrate the broad applicability for solving analytical problems.

■ AUTHOR INFORMATION

Corresponding Author

John C. Wright – Department of Chemistry, University of Wisconsin-Madison, Madison, Wisconsin 53706, United States;
orcid.org/0000-0002-6926-1837; Email: wright@chem.wisc.edu

Complete contact information is available at:

<https://pubs.acs.org/10.1021/acs.analchem.0c01662>

Notes

The author declares no competing financial interest.

■ ACKNOWLEDGMENTS

The ideas in this paper were supported by the National Science Foundation under grant CHE-1709060.

■ REFERENCES

- (1) Wright, J. C. *Int. Rev. Phys. Chem.* **2002**, *21*, 185–255.
- (2) Wright, J. C. *Annu. Rev. Anal. Chem.* **2017**, *10*, 45–70.
- (3) Castelvecchi, D. *Nature* **2018**, *561*, 446.
- (4) Wright, J. C. *Springer Ser. Opt. Sci.* **2019**, *226*, 145.
- (5) Wright, J. C. *Chem. Phys. Lett.* **2016**, *662*, 1–13.
- (6) Zhao, W.; Wright, J. C. *J. Am. Chem. Soc.* **1999**, *121*, 10994–10998.
- (7) Rabenstein, D. L. *Anal. Chem.* **2001**, *73*, 214A.
- (8) Boyer, T. H. *Ann. Phys.* **1970**, *56*, 474–503.
- (9) Munowitz, M.; Pines, A. *Advances in Chemical Physics* **1986**, *66*, 1–152.
- (10) Maker, P. D.; Terhune, R. W. *Phys. Rev.* **1965**, *137* (3A), A801.
- (11) Zhao, W.; Wright, J. C. *Phys. Rev. Lett.* **2000**, *84*, 1411–1414.
- (12) Hybl, J. D.; Albrecht, A. W.; Gallagher Faeder, S. M.; Jonas, D. M. *Chem. Phys. Lett.* **1998**, *297*, 307–313.
- (13) Sowley, H.; Liu, Z.; Davies, J.; Peach, R.; Guo, R.; Sim, S.; Long, F.; Holdgate, G.; Willison, K.; Zhuang, W.; Klug, D. R. *J. Phys. Chem. B* **2019**, *123* (17), 3598–3606.
- (14) Zhao, W.; Wright, J. C. *Phys. Rev. Lett.* **1999**, *83*, 1950–1953.
- (15) Donaldson, P. M.; Guo, R.; Fournier, F.; Gardner, E. M.; Barter, L. M. C.; Barnett, C. J.; Gould, I. R.; Klug, D. R.; Palmer, D. J.; Willison, K. R. *J. Chem. Phys.* **2007**, *127* (11), 114513.
- (16) Donaldson, P. M.; Guo, R.; Fournier, F.; Gardner, E. M.; Gould, I. R.; Klug, D. R. *Chem. Phys.* **2008**, *350* (1–3), 201–211.
- (17) Fournier, F.; Gardner, E. M.; Guo, R.; Donaldson, P. M.; Barter, L. M. C.; Palmer, D. J.; Barnett, C. J.; Willison, K. R.; Gould, I. R.; Klug, D. R. *Anal. Biochem.* **2008**, *374* (2), 358–365.
- (18) Fournier, F.; Gardner, E. M.; Kedra, D. A.; Donaldson, P. M.; Guo, R.; Butcher, S. A.; Gould, I. R.; Willison, K. R.; Klug, D. R. *Proc. Natl. Acad. Sci. U. S. A.* **2008**, *105* (40), 15352–15357.
- (19) Carlson, R. J.; Wright, J. C. *J. Mol. Spectrosc.* **1990**, *143*, 1–17.
- (20) Hurst, G. B.; Wright, J. C. *J. Chem. Phys.* **1991**, *95*, 1479–1486.
- (21) Riebe, M. T.; Wright, J. C. *Chem. Phys. Lett.* **1987**, *138*, 565–570.
- (22) Boyle, E. S.; Neff-Mallon, N. A.; Wright, J. C. *J. Phys. Chem. A* **2013**, *117* (047), 12401–12408.
- (23) Boyle, E. S.; Pakoulev, A. V.; Wright, J. C. *J. Phys. Chem. A* **2013**, *117* (27), 5578–5588.
- (24) Boyle, E. S.; Neff-Mallon, N. A.; Handali, J. D.; Wright, J. C. *J. Phys. Chem. A* **2014**, *118* (17), 3112–3119.
- (25) Handali, J. D.; Sunden, K. F.; Thompson, B. J.; Neff-Mallon, N. A.; Kaufman, E. M.; Brunold, T. C.; Wright, J. C. *J. Phys. Chem. A* **2018**, *122*, 9031.
- (26) Tolles, W. M.; Nibler, J. W.; McDonald, J. R.; Harvey, A. B. *Appl. Spectrosc.* **1977**, *31* (4), 253–271.
- (27) Begley, R. F.; Harvey, A. B.; Byer, R. L. *Appl. Phys. Lett.* **1974**, *25* (7), 387–390.
- (28) Tolles, W. M.; Nibler, J. W.; McDonald, J. R.; Harvey, A. B. *Appl. Spectrosc.* **1977**, *31*, 253–271.
- (29) Chen, P. C.; Gomes, M. J. *Phys. Chem. A* **2008**, *112* (14), 2999–3001.
- (30) Zanni, M. T.; Asplund, M. C.; Hochstrasser, R. M. *J. Chem. Phys.* **2001**, *114*, 4579–4590.
- (31) Wright, J. C. *J. Phys. Chem. Lett.* **2019**, *10* (11), 2767–2774.
- (32) Kamga, F. M.; Sceats, M. G. *Opt. Lett.* **1980**, *5*, 126–128.
- (33) Wright, J. C. *J. Phys. Chem. Lett.* **2019**, *10*, 2767.
- (34) Neff-Mallon, N. A.; Wright, J. C. *Anal. Chem.* **2017**, *89* (24), 13182–13189.
- (35) Volkmer, A.; Cheng, J.-X.; Sunney Xie, X. *Phys. Rev. Lett.* **2001**, *87* (2), 023901.
- (36) Hoffman, D. P.; Mathies, R. A. *Acc. Chem. Res.* **2016**, *49* (4), 616–625.
- (37) Mathew, N. A.; Yurs, L. A.; Block, S. B.; Pakoulev, A. V.; Kornau, K. M.; Sibert, E. L.; Wright, J. C. *J. Phys. Chem. A* **2010**, *114* (2), 817–832.